Environ. Sci. Technol. **1998**, *32,* 3218−3223

Laser Desorption/Ionization of Single Ultrafine Multicomponent Aerosols

ZHAOZHU GE,[†]
ANTHONY S. WEXLER,*[,†] AND
MURRAY V. JOHNSTON[‡]

Department of Mechanical Engineering and Department of Chemistry and Biochemistry, University of Delaware, Newark, Delaware 19716

Laser desorption/ionization characteristics of single ultrafine multicomponent aerosols have been investigated. The results confirm earlier findings that (a) the negative ion spectra are dominated by free electrons and (b) the ion yield-to-mass ratio is higher for ultrafine particles than that of larger ones. The smallest relative mass of KCl detected in NaCl is about 0.06%, which corresponds to 10^{-20} g of KCl in a 50-nm particle. Experimental results from mixtures of KCl/NaCl and NaCl/NH_4NO_3 show that, by measuring the peak area ratio of certain ions in the spectrum, the total composition can be inferred. The experimental results also show that ion yields vary with composition even for ultrafine particles, making multicomponent analysis of complex particles difficult. A simple model is developed to quantify the relationship between ion yield and particle composition. Using this model, a relative ion yield of 4.9 is found for K^+ from KCl over Na^+ from NaCl, while 4.4 is found for Na^+ from NaCl over NO^+ from NH_4NO_3. It has been shown that analyzing particles composed of chemicals with common cations but different anions, such as NaCl/$NaNO_3$ from positive ion spectra, is also possible. The ability of laser desorption/ionization to detect trace metals is studied. With relative mass of each element on the order of 1%, which corresponds to the absolute mass of the order of 10^{-17} g in a 60-nm particle, strong peaks of Na^+, Mg^+, K^+, Cr^+, Fe^+, Cu^+, Zn^+, Cd^+, Cs^+, La^+, and Pb^+ are observed in the spectrum. The smallest amount detectable for some easily ionizable elements, such as K and Cs, should be much lower than 1%. Although no ion yield is observed for pure $(NH_4)_2SO_4$ particles, peaks of S^+ and SO^+ associated with $(NH_4)_2SO_4$ are shown in spectrum from mixtures of $(NH_4)_2SO_4$, NH_4NO_3, and several trace metals. The application of laser desorption/ionization to measuring atmospheric ultrafine aerosols is also discussed.

Introduction

Analyzing the chemical composition of ultrafine aerosol particles with diameters below 100 nm is important in understanding condensation processes during combustion and nucleation processes in photochemical systems, which in turn helps elucidate other processes affecting air pollution control, climate change, and human health. Conventionally, chemical characterization of aerosol particles requires that a sufficient sample be collected on a substrate prior to analysis. In addition to possible contamination and evaporation of volatile compounds during sampling, collection of sufficient ultrafine particle mass tends to be very time-consuming and thus limits temporal resolution. Also, particle-to-particle composition variations are usually not available.

In recent years, a new on-line analytical method based on laser desorption/ionization has been developed that is capable of analyzing single aerosol particles [reviewed by Johnston and Wexler (*1*)]. Briefly, the aerosol is sampled directly into the source region of a time-of-flight mass spectrometer through a differentially pumped inlet. The resulting particle beam intercepts a continuous helium−cadmium laser beam, and the scattered radiation pulse from each particle triggers an excimer laser so the particle is ablated in-flight. The resulting ions are accelerated into the mass spectrometer and analyzed. Since the time between sampling and analysis is approximately 1 ms, chemical transformation of the particles during sampling is minimized. With such excellent time resolution and the capability of analyzing volatile compounds, this type of instrumentation has been used in monitoring real-time chemical reactions (*2*), in studying chemical and physical aerosol processes such as deliquescence and crystallization (*3*−*6*), and in probing the chemical composition of aerosol particles in the ambient atmosphere (*7*−*9*). Extensive laboratory tests of the instrument have also been performed (*10*, *11*).

Since light scattering is used to detect individual particles, those that are much smaller than the wavelength of the radiation cannot be detected. Usually, the instrument is limited to particles greater than 0.2 μm. To identify the sources of ultrafine particles relevant to semiconductor processing, Reents et al. (*12*) used a similar apparatus but without detection. They freely fired the excimer laser and hit the particles randomly. In this way, particles as small as 20 nm have been analyzed. Carson et al. (*13*) borrowed this idea and constructed a similar instrument that has detected even smaller particles. Both instruments suffer from a relatively low ablation rate, largely due to dispersion of the particle beam in the source region. Recently, a new size-selective inlet has been developed that is capable of focusing the particle beam to the laser focal point, thus improving ablation rate significantly (*14*). In this work, we couple the new inlet with the instrument developed by Carson et al. (*13*), called RSMS−II (Rapid Single-particle Mass Spectrometry, Version II), to analyze ultrafine multicomponent aerosol particles generated in the laboratory.

Almost all the aerosol particles in the atmosphere are multicomponent aerosols. The ability of these laser desorption/ionization methods to monitor the chemical composition of atmospheric aerosols has been demonstrated by a number of groups (*7*−*9*). In their field measurements, chemical composition with size information was measured for particles larger than 0.3 μm. But most of the particles that play an important role in climate change, air pollution control, and human health are nucleation, Aitken, and accumulation particles and reside in the 10−200-nm size range. The ultimate application of RSMS−II is to measure the chemical composition of these individual aerosol particles in the ambient environment. Thus prior to field application, laboratory studies must be performed to understand (a) how the laser desorption/ionization process affects the characterization of each compound in ultrafine multicomponent aerosols and (b) the detection limits for atmospherically relevant compounds. Ultrafine aerosols of pure NaCl, KCl, and NH_4NO_3 have been investigated by Carson et al. (*13*) using an instrument similar to RSMS−II. Their results show

* Corresponding author phone: (302)831-8743; fax: (302)831-3619; e-mail: wexler@me.Udel.edu.
[†] Department of Mechanical Engineering.
[‡] Department of Chemistry and Biochemistry.

S0013-936X(98)00104-7 CCC: $15.00
Published on Web 08/25/1998

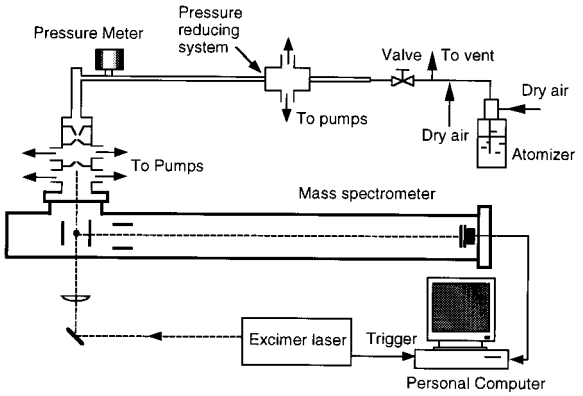

FIGURE 1. Schematic of experimental setup.

that, although positive ion mass spectra of ultrafine particles are similar to micron-size particles, the negative ion mass spectra are dominated by free electrons instead of atomic or molecular ions. Also, they observed that, relative to total mass, small particles tend to produce a much higher ion yield than large particles. Reents et al. (*12*) tested their instrument with multicomponent aerosols of $CsNO_3$, $RbNO_3$, $(NH_4)_2SO_4$, CsCl, RbCl, NaCl, KCl, and talc.

In this work, laser desorption/ionization characteristics of ultrafine multicomponent aerosol particles are studied, and the differences between the spectra from these particles and those on the micron-size range are investigated. Aerosols generated from different known mixtures of atmospherically relevant chemicals are analyzed, and detection limits of each compound are investigated. From these experiments, a knowledge base of laser desorption/ionization processes for these compounds and their mixtures is accumulated, which can then be applied in future field studies.

Experimental Section

The experimental setup shown in Figure 1 is similar to the apparatus described in Carson et al. (*13*) but with improvements in inlet and data acquisition system. Polydisperse aqueous droplets were produced from an atomizer (model 3075, TSI, St. Paul, MN) that contains solutions of known composition. The flow and droplets were mixed with a dry airstream to remove solvent (water for this work). The resulting dry particles were sent to an inlet that transports the particles from atmospheric pressure to the source region of a time-of-flight mass spectrometer. Particle inertia was utilized in the design of the inlet to focus only a narrow size range to the laser focus. By manipulating the pressure at the nozzle, particles of a selected size entered the source region and were ablated with a freely firing 193-nm excimer laser (model PSX-100, MPB Technologies, Dorval, Quebec, Canada).

Unlike the traditional on-line laser desorption/ionization apparatus, in which the excimer laser beam intersects the particle beam orthogonally, the excimer laser beam was configured to be collinear with the particle beam but propagated in the opposite direction to maximize the ablation rate. The laser freely fired at frequencies up to 100 Hz. It was estimated that, for the current configuration, the chance of hitting two particles simultaneously is less than 10^{-4}. The laser pulse energy was maintained at 2.5 mJ. Only those particles residing in a 4 cm long by 600 μm wide region near the laser beam focus were ablated and analyzed (*13*). Ions generated by laser desorption/ionization were accelerated to a linear time-of-flight mass spectrometer and detected with a dual microchannel plate detector. The output signal was sampled with a custom-built 500 MHz data acquisition board (model 9847, Precision Instruments, Knoxville, TN) mounted in a personal computer.

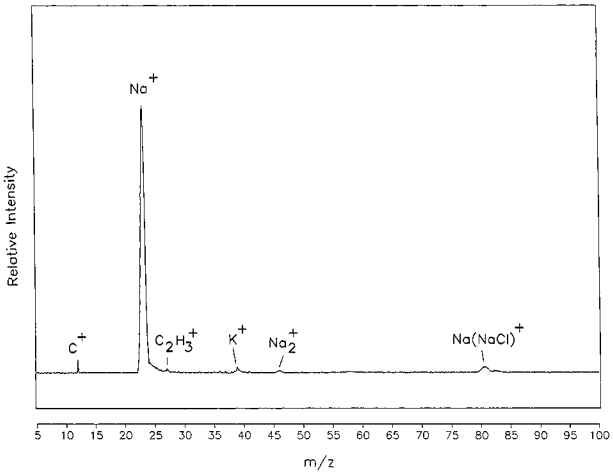

FIGURE 2. Averaged positive ion spectra of 40 particles dried from aqueous droplets of a NaCl/KCl mixture with $X_{KCl} = 0.2\%$. Particle diameters are around 50 nm.

The data acquisition board was triggered by each firing of the excimer laser. The excimer laser was freely fired at 15 Hz. Most laser shots missed particles and resulted in spectra that were null. The board checked if the maximum ion current in each sampling cycle exceeded a user-programmable threshold. If the ion current for a sample was above threshold, a flag signaled that a valid spectrum was recorded. A program on the personal computer checked this flag and saved the corresponding data in disk. Therefore, each spectrum saved corresponded to a particle being ablated by the excimer laser.

It has been shown that particles in the 12−150-nm size range, when laser ablated, usually do not yield negative ions for almost all compositions (*13*). We have confirmed the earlier conclusion of Carson et al. (*13*) that electrons were preferentially emitted. In this work, spectra were only obtained in the positive ion mode.

Results and Discussion

Figure 2 shows a spectrum from a NaCl and KCl mixture with a mole fraction of $X_{KCl} = 0.2\%$ ($X_{KCl} = m_{KCl}/(m_{KCl} + m_{NaCl})$). The particle diameter was estimated to be around 50 nm. The absolute amount of KCl (m_{KCl}) in the particle is given by

$$m_{KCl} = \frac{\frac{4}{3}\pi r^3 \rho_p X_{KCl} M_{KCl}}{X_{KCl} M_{KCl} + (1 - X_{KCl}) M_{NaCl}} \qquad (1)$$

where r is the radius of the particle, ρ_p is the particle density, M_{KCl} and M_{NaCl} are the molar masses of KCl and NaCl. For the particles shown in Figure 2, considering the small amount of KCl in the particles, the density of the particle can be approximated by the density of NaCl. Thus the absolute amount of KCl in the 50 nm-particle is about 10^{-18} g. NaCl and KCl have been studied extensively by laser desorption/ionization because of their ease of ionization (*2*−*4*, *15*), and Na and K are two common elements observed in atmospheric aerosols. In Figure 2, the K^+ peak (m/z 39 and 41) can be positively identified. Other peaks indicate common ions from NaCl corresponding to Na^+ (m/z 23), Na_2^+ (m/z 46), and $Na(NaCl)^+$ (m/z 81). The C^+ and $C_2H_3^+$ peaks may be attributed to organic contamination during aerosol preparation (*12*, *16*). The K^+ peak can even be identified in the spectrum of a 50-nm particle from an $X_{KCl} = 0.05\%$ mixture, in which the absolute amount of KCl is only about 10^{-20} g and the relative mass of KCl is about 0.06%.

The smallest amount detected for KCl is similar to laser microprobe mass spectrometry (LAMMS), which is on the

order of 10^{-19} g (*17*). Note that the sample size, laser wavelength, and pulse energy applied were different in LAMMS. For example, the laser wavelength was 266 nm for LAMMS and 193 nm for current work. The relative mass of KCl detected is about 0.06%, which is considerably larger than that of LAMMS due to the much smaller particle mass. We also observed that the intensity of ions of ultrafine particles is on the same order as that of micron-size particles (*3*), which confirms the finding of Carson et al. (*13*) that the ion yield-to-mass ratio for ultrafine particles is higher than large particles.

Ge et al. (*3*) studied the surface chemical composition of micron-size particles dried from NaCl and KCl mixed solutions with different mole fractions. They found that the dry particles do not have a homogeneous chemical morphology except at the eutonic point. The particles are composed of a pure salt core surrounded by a mixed salt coating, where the composition of the pure salt core is solely determined by the original aerosol composition, but the coating is identical in chemical composition to the eutonic point and is independent of the original component mole fractions. Since most atmospheric aerosols are multicomponent aerosols, during their life cycle, they may experience physical processes such as crystallization and deliquescence as ambient relative humidity changes. Thus, it is possible that a shell-core structure may be formed as a result of these processes. Evidences in field measurements also indicated a shell-core structure for both submicron and micron particles (*18*).

It is well-known that for micron-size particles only a small fraction of the particle volume is vaporized by laser desorption (*2*−*4*). Considering possible structured morphology and heterogeneous distribution of chemical compounds inside atmospheric aerosols, during field measurements of chemical composition of micron-size particles using laser desorption/ionization, the data probably include a bias toward the surface composition of aerosol particles rather than the total.

The situation is different for laser desorption/ionization of ultrafine aerosol particles. Carson et al. (*13*) speculated that because of the small particle size a greater fraction of the particle is vaporized and ionized as compared to micron-size particles. They observed higher ion yield-to-mass ratio for ultrafine particles, which was confirmed in our current study of the detection limits of KCl in NaCl particles. To examine whether the surface characteristics of laser desorption/ionization affects composition measurements of ultrafine multicomponent aerosols, mixtures of KCl and NaCl with different mole fractions were investigated. Figure 3 shows a plot of peak area ratio $[K^+]/([K^+] + [Na^+])$ versus mole fraction X_{KCl}. Each data point represents the average of at least 40 spectra of identical particles. The error bars indicate standard error of the mean. The peak area ratio increases monotonically as mole fraction increases. Rather than a linear relationship between peak area ratio and mole fraction that we expected for a total volume composition, the slope of the curve decreases as mole fraction X_{KCl} increases, which reveals an important characteristic of laser desorption/ionization: different matrix materials ionize with different yields. In this case, the ion yield of KCl is higher than that of NaCl. To understand this phenomenon quantitatively, a simple model has been developed. Consider a particle containing two components, with mole number m_a and m_b and ion yield of i_a and i_b, respectively. The peak area ratio, (R_p), corresponding to the ratio of intensity of the ions associated with each component ($[K^+]/([K^+] + [Na^+])$ in this case), can be expressed as

$$R_p = \frac{i_a m_a}{i_a m_a + i_b m_b} \tag{2}$$

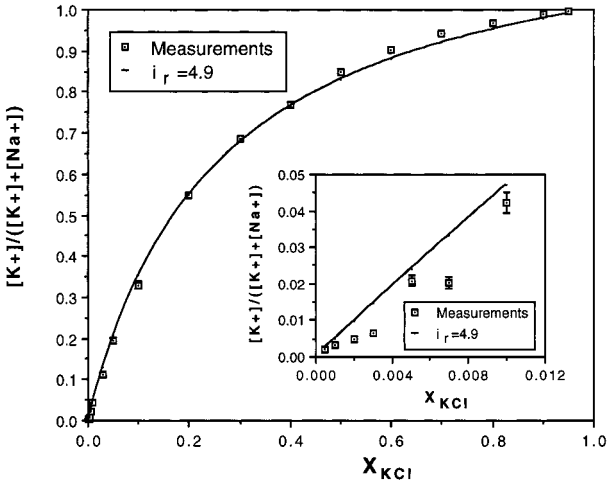

FIGURE 3. Peak area ratio of $[K^+]/([K^+] + [Na^+])$ versus mole fraction X_{KCl}. Particle diameters are around 50 nm. Each data point is the average of at least 40 spectra. The error bars indicate the standard error of the mean. The model with $i_r = 4.9$ is also shown.

By introducing a relative ion yield i_r defined as i_a/i_b, and a mole fraction x (X_{KCl} in this case) defined as $m_a/(m_a + m_a)$, eq 2 can be simplified to

$$R_p = \frac{i_r x}{1 + (i_r - 1)x} \tag{3}$$

Note that i_r is defined similarly to the relative sensitivity factors (RSF) employed in LAMMS for quantitative analysis (*19*−*21*). The change in peak area ratio R_p with mole fraction x can be determined by

$$\frac{dR_p}{dx} = \frac{i_r}{(1 + (i_r - 1)x)^2} \tag{4}$$

From eq 4, dR_p/dx decreases as x (i.e., X_{KCl}) increases as long as $i_r > 1$, which complies exactly to what we observe in Figure 3. The value of i_r can be approximated from the experiment data. For this system, i_r is found to be 4.9, which means that the ion yield of K^+ from KCl is about 4.9 times that of Na^+ from NaCl. The same relative ion yield was found to be about 4.2 using LAMMS (*20*) and about 4.0 in micron-size particle analysis (*3*). Note that the difference may be due to the different laser wavelength employed in LAMMS (266 nm), micron-size particle analysis (248 nm), and current studies (193 nm). A curve from the model with $i_r = 4.9$ is also plotted in Figure 3.

Figure 4 shows a spectrum of a $NaCl/NH_4NO_3$ mixture with a mole fraction $X_{NaCl} = 1\%$ ($X_{NaCl} = m_{NaCl}/(m_{NaCl} + m_{NH_4NO_3})$). The particle diameter was estimated to be around 60 nm. The absolute amount of Na in the particle was about 10^{-17} g. The Na^+ peak (m/z 23) can be positively identified. Other peaks indicate NO^+ (m/z 30) from NH_4NO_3 and C^+ (m/z 12) from organic contamination during aerosol preparation (*12*, *16*). It is also noteworthy, on examining Figure 4, that the positive ions NO^+ indicate nitrate anions from NH_4NO_3. In contrast, the expected NH_4^+ peak is very weak and hardly observable.

Experiments similar to those for the NaCl and KCl mixtures were performed to investigate the laser desorption/ionization process for NaCl and NH_4NO_3 mixtures. The diameters of the particles were around 60 nm. The peak area ratio $[Na^+]/([Na^+] + [NO^+])$ versus mole fraction X_{NaCl} is plotted in Figure 5. The data indicate that a total volume composition was measured. Again, we observe a difference in ion yield between the two components. For this system, the relative

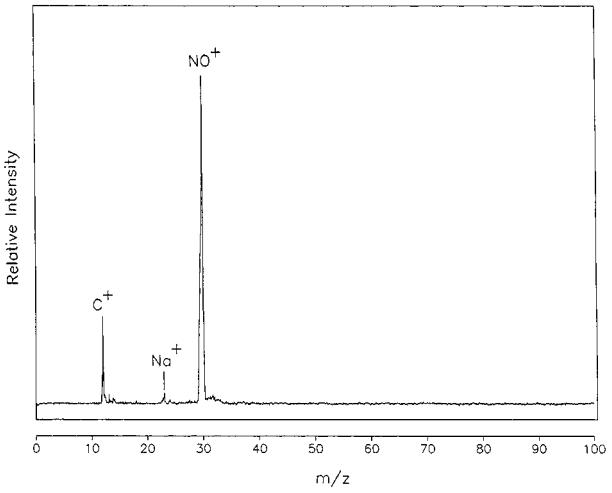

FIGURE 4. Positive ion spectrum of a single particle dried from an aqueous droplet of a NaCl/NH_4NO_3 mixture with $X_{NaCl} = 2\%$. Particle diameter is around 60 nm.

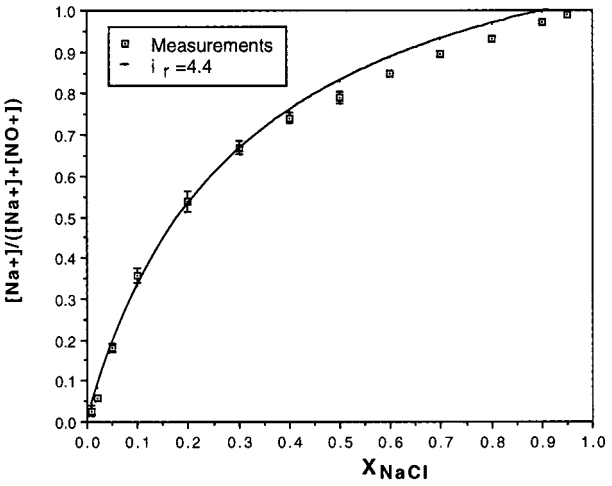

FIGURE 5. Peak area ratio of $[Na^+]/([Na^+] + [NO^+])$ versus mole fraction X_{NaCl}. Particle diameters are around 60 nm. Each data point is the average of at least 40 spectra. The error bars indicate the standard error of the mean. The model with $i_r = 4.4$ is also shown.

ion yield of Na^+ from NaCl over NO^+ from NH_4NO_3 (i_r in eq 3) is determined to be about 4.4, which is also shown in Figure 5.

Mixtures of $NaNO_3$/NaCl were studied to investigate the ability to analyze particles composed of chemicals with common cations but different anions. Such measurements are difficult since only positive mode spectra are obtainable for ultrafine particles. But for the mixtures of NaCl/NH_4NO_3, positive ions such as NO^+ indicate anions in the particles, and peaks of Na^+ and NO^+ can be identified in the spectra of pure $NaNO_3$ particles where the peak area ratio $[Na^+]/[NO^+]$ was measured to be 5.3. Figure 6 shows a spectrum of a NaCl/$NaNO_3$ mixture with mole fraction $X_{NaNO_3} = 5\%$ ($X_{NaNO_3} = m_{NaNO_3}/(m_{NaCl} + m_{NaNO_3})$). The diameters of the particles were around 60 nm. The NO^+ (m/z 30) peak can be positively identified. Other peaks indicate Na^+ (m/z 23) from both NaCl and $NaNO_3$ and indicate C^+ (m/z 12) from organic contamination during aerosol preparation (*12, 16*). A peak at m/z 46 is most likely Na_2^+ rather than NO_2^+ since the particle was NaCl abundant.

The peak area ratio $[NO^+]/[Na^+]$ versus mole fraction X_{NaNO_3} for $NaNO_3$/NaCl mixtures is plotted in Figure 7. The result is similar to that of the other two mixtures but more complicated to interpret because the Na^+ peak is attributed

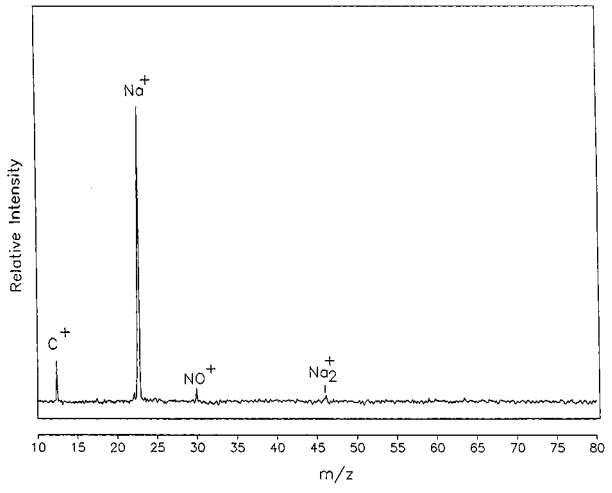

FIGURE 6. Positive ion spectrum of a single particle dried from an aqueous droplet of a NaCl/$NaNO_3$ mixture with $X_{NaNO_3} = 5\%$. Particle diameter is around 60 nm.

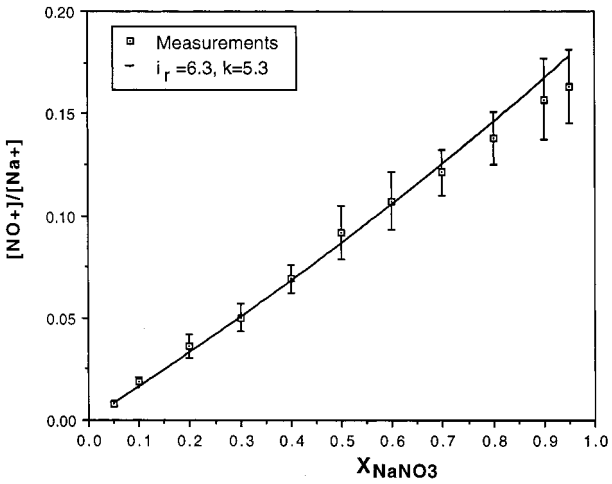

FIGURE 7. Peak area ratio of $[NO^+]/[Na^+]$ versus mole fraction X_{NaNO_3}. Particle diameters are around 60 nm. Each data point is the average of at least 40 spectra. The error bars indicate the standard error of the mean. The model with $i_r = 6.3$ is also shown.

to both NaCl and $NaNO_3$. The peak area ratio $[NO^+]/[Na^+]$ can be expressed as

$$\frac{[NO^+]}{[Na^+]} = \frac{x}{i_r(1 - x) + kx} \qquad (5)$$

where x is the mole fraction of $NaNO_3$ (X_{NaNO_3}), i_r indicates the relative ion yield of Na^+ from NaCl over NO^+ from $NaNO_3$, and k indicates the peak area ratio $[Na^+]/[NO^+]$ of pure $NaNO_3$ particles and was measured to be 5.3. The i_r is determined to be about 6.3, which is also shown in Figure 7.

Quantitation of chemical species in an ultrafine multicomponent aerosol using laser desorption/ionization is possible if the relative ion yield of each component to a reference compound is known. For atmospheric aerosols, the reference compound must have several properties: (a) a unique peak that is positively identifiable, (b) ease of ionization, and (c) ubiquitous in atmospheric aerosols. Alkali metal salts (NaCl, KCl) are relatively easy to ionize and have unique identifiable atomic peaks (Na^+, K^+). The alkali metal salts reside primarily in the coarse size mode, usually sea spray aerosols. Recent field measurements using laser desorption/ionization found that potassium was present in most submicron particles and that sodium was also present

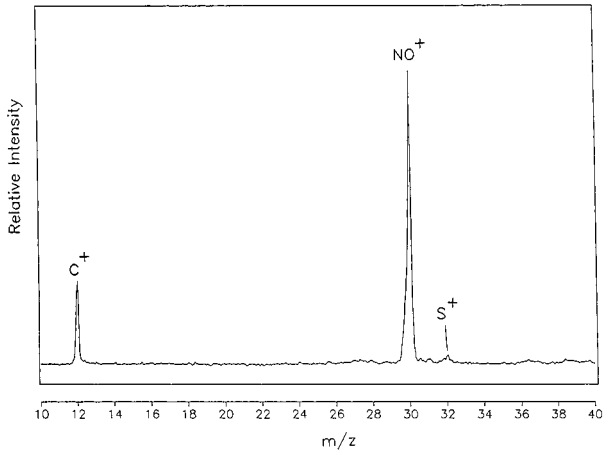

FIGURE 8. Positive ion spectrum of a single particle dried from an aqueous droplet of a $(NH_4)_2SO_4/NH_4NO_3$ mixture with mole ratio of 1:1. Particle diameter is around 60 nm.

in submicron particles, but not as often as potassium (*7*). Therefore, alkali metals may serve as references for quantitative analysis of ultrafine atmospheric aerosols. NH_4NO_3 is also easy to ionize and is a major component of atmospheric aerosols. But its primary peak is at m/z 30 corresponding to NO^+, which may be difficult to distinguish from CH_4N^+ or CH_2O^+ if organic compounds are present (*7*).

$(NH_4)_2SO_4$ is expected to be one of the key component in ultrafine atmospheric aerosols. The formation of $(NH_4)_2SO_4$ is a result of neutralization of H_2SO_4 particles in nucleation or Aitken mode by NH_3. $(NH_4)_2SO_4$ was also found on the surface of soot particles in field measurements (*18*). $(NH_4)_2SO_4$ is thus considered to be ubiquitous in ultrafine atmospheric aerosols. Pure $(NH_4)_2SO_4$ aerosols in the size range 40−60 nm were analyzed with laser desorption/ionization, but no ion yield was observed. Figure 8 shows a spectrum of a $(NH_4)_2SO_4$ and NH_4NO_3 mixture with a mole ratio of 1:1. The diameter of the particles was estimated to be around 60 nm. The C^+ peak may be attributed to organic contamination during aerosol preparation (*12, 16*). NH_4NO_3 gave ions corresponding to NO^+. A weak peak at m/z 32 corresponding to S^+ is observed in this spectrum but only occasionally appears in other spectra we collected.

Effective detection of $(NH_4)_2SO_4$ in ultrafine aerosols using laser desorption/ionization is therefore difficult from the results of these laboratory experiments. But real atmospheric ultrafine aerosols usually contain ammonium, sulfate, nitrate, alkali metals, elemental carbon, organics, and trace metals. Some components, especially trace metals, may ease the detection of $(NH_4)_2SO_4$. Using a similar apparatus as employed in this work, Reents et al. (*12*) observed ions corresponding to S^+, SO^+, SO_2^+, SO_3^+, $(NH_4)HSO_4^+$, and even $(NH_4)_2SO_4^+$ from $(NH_4)_2SO_4$. The particles were mixtures of $(NH_4)_2SO_4$, and talc (silica and magnesium silicate). It is not known whether silicon or magnesium initiated the emission of ions from $(NH_4)_2SO_4$.

The ability of laser desorption/ionization to detect trace metals in ultrafine aerosols were also investigated. Figure 9 shows the mass spectrum of a single aerosol particle produced from mixtures of NH_4NO_3 and several metal salts. The particle size was estimated to be around 60 nm. The mole fractions of each component were 93.5% NH_4NO_3, 0.93% each for $NaNO_3$, KNO_3, $Cr(NO_3)_3$, $Fe(NO_3)_3$, $Cd(NO_3)_2$, $La(NO_3)_3$, and $Pb(NO_3)_2$. Three types of ions are observed: C^+ (m/z 12) from organic contamination during aerosol preparation (*12, 16*), ions from NH_4NO_3 corresponding to NO^+ (m/z 30), and bare atomic metal ions (Na^+, K^+, Cr^+, Fe^+, Cd^+, La^+, and Pb^+). A peak at m/z 70 is also observed, which may

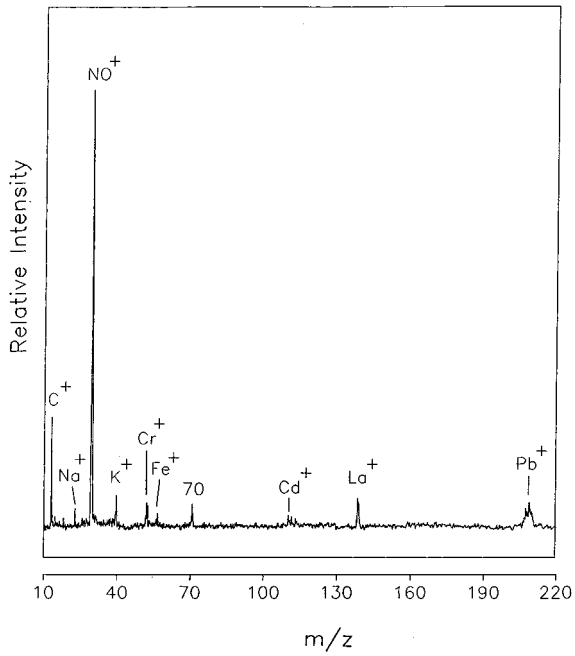

FIGURE 9. Positive ion spectrum of single aerosol particle produced from mixtures of NH_4NO_3 and several metal salts. The particle size is around 60 nm. The mole fractions of each component were 93.5% NH_4NO_3, 0.93% each for $NaNO_3$, KNO_3, $Cr(NO_3)_3$, $Fe(NO_3)_3$, $Cd(NO_3)_2$, $La(NO_3)_3$, $Pb(NO_3)_2$.

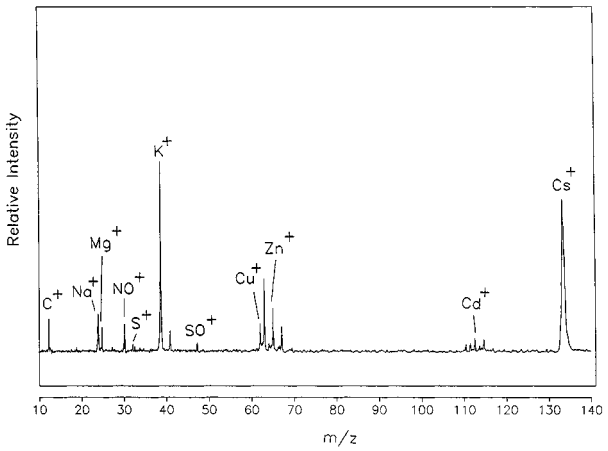

FIGURE 10. Positive ion spectrum of single aerosol particle produced from mixtures of $(NH_4)_2SO_4$, NH_4NO_3, and several metal salts. The particle size is around 60 nm. The mole fractions of each component were 74.6% $(NH_4)_2SO_4$, 14.9% NH_4NO_3, 1.5% each for NaCl, KCl, $CuSO_4$, $ZnCl_2$, $MgSO_4$, $Cd(NO_3)_2$, and CsCl.

be $Cr{\cdot}H_2O^+$. The relative mass of each metal element is about 1%, while the absolute amount is on the order of 10^{-17} g.

Due to the fact that $(NH_4)_2SO_4$ is ubiquitous in most ultrafine atmospheric aerosol particles, the detection of trace metals in an $(NH_4)_2SO_4$ abundant particle was also studied. Also, as we have pointed out previously, some trace metals may incite the emission of ions from $(NH_4)_2SO_4$. A mass spectrum from a single aerosol particle containing $(NH_4)_2SO_4$, NH_4NO_3, and several metal salts is shown in Figure 10. The particle size was estimated to be around 60 nm. The mole fractions of each component were 74.6% $(NH_4)_2SO_4$, 14.9% NH_4NO_3, and 1.5% each for NaCl, KCl, $CuSO_4$, $ZnCl_2$, $MgSO_4$, $Cd(NO_3)_2$, and CsCl. Four types of ions are observed: C^+ (m/z 12) from organic contamination during aerosol preparation (*12, 16*), ions from NH_4NO_3 corresponding to NO^+ (m/z 30), bare atomic metal ions (Na^+, Mg^+, K^+, Cu^+, Zn^+, Cd^+, and Cs^+), and surprisingly, S^+ and SO^+ from

$(NH_4)_2SO_4$. Note that the peaks due to Cs and K are considerably larger, which indicates that laser desorption/ionization may be able to detect much lower amounts of these in atmospheric aerosol particles. Ions of S^+ and SO^+ are also observed in spectra from mixtures of $(NH_4)_2SO_4$ and the same metal salts, but without the NH_4NO_3.

Acknowledgments

The authors thank R. Mallina for technical assistance throughout this work. This research was supported by grants from the National Science Foundation (ATM-9422993) and the Environmental Protection Agency (R82-2980-010).

Literature Cited

(1) Johnston, M. V.; Wexler, A. S. *Anal. Chem*. **1995**, *67*, 721A−726A.
(2) Carson, P. G.; Johnston, M. V.; Wexler, A. S. *Aerosol Sci. Technol*. **1997**, *26*, 291−300.
(3) Ge, Z.; Wexler, A. S.; Johnston, M. V. *J. Colloid Interface Sci*. **1996**, *183*, 68−77.
(4) Ge, Z.; Wexler, A. S.; Johnston, M. V. *J. Phys. Chem*. **1998**, *102*, 173−180.
(5) Neubauer, K. R.; Johnston, M. V.; Wexler, A. S. *Int. J. Mass Spectrom. Ion Processes* **1997**, *163*, 29−37.
(6) Neubauer, K. R.; Johnston, M. V.; Wexler, A. S. Humidity effects on mass spectra of single aerosol particles. *Atmos. Environ*. **1998**, *32*, 2521−2529.
(7) Murphy, D. M.; Thomson, D. S. *J. Geophys. Res*. **1997**, *102*, 6341−6352.
(8) Murphy, D. M.; Thomson, D. S. *J. Geophys. Res*. **1997**, *102*, 6353−6368.
(9) Liu, D. Y.; Rutherford, D.; Kinsey, M.; Prather, K. A. *Anal. Chem*. **1997**, *69*, 1808−1814.
(10) Mansoori, B. A.; Johnston, M. V.; Wexler, A. S. *Anal. Chem*. **1994**, *66*, 3681−3687.
(11) Neubauer, K. R.; Johnston, M. V.; Wexler, A. S. *Int. J. Mass Spectrom. Ion Processes* **1995**, *151*, 77−87.
(12) Reents, W. D.; Downey, S. W.; Emerson, A. B.; Mujsce, A. M.; Muller, A. J.; Siconolfi, D. J.; Sinclair, J. D.; Swanson, A. G. *Aerosol Sci. Technol*. **1995**, *23*, 263−270.
(13) Carson, P. G.; Johnston, M. V.; Wexler, A. S. *Rapid Commun. Mass Spectrom*. **1997**, *11*, 993−996.
(14) Mallina, R. V. Rapid Single-particle Mass Spectrometry (RSMS): inlet design and analysis. Ph.D. Dissertation, University of Delaware, 1998.
(15) Thomson, D. S.; Murphy, D. M. *Appl. Opt*. **1993**, *32*, 6818−6826.
(16) Middlebrook, A. M.; Thomson, D. S.; Murphy, D. M. *Aerosol Sci. Technol*. **1997**, *27*, 293−307.
(17) Fletcher, R. A.; Small, J. A. In *Aerosol Measurement: Principles, Techniques and Applications*; Willeke, K., Baron, P. A., Eds.; Van Nostrand Reinhold: New York, 1992.
(18) Goschnick, J.; Schuricht, J.; Ache, H. J. *Fresenius J. Anal. Chem*. **1994**, *350*, 426−430.
(19) Musselman, I. H.; Simons, D. D.; Linton, R. W. In *Microbeam Analysis*; Newbury, D. E., Ed.; San Francisco Press: San Francisco, 1988.
(20) Otten, Ph.; Bruynseels, F.; Van Grieken, R. *Anal. Chim. Acta* **1987**, *195*, 117−124.
(21) Bate, D. J.; Leake, J. A.; Matthews, L. J.; Wallach, E. R. *Int. J. Mass Spectrom. Ion Processes* **1993**, *127*, 85−93.

Received for review February 2, 1998. Revised manuscript received July 6, 1998. Accepted July 9, 1998.

ES980104Y